International Journal of Pure and Applied Mathematics
Volume 51 No. 4 2009, 537-556

NUMERICAL EXPERIMENT ON CONFORMAL MAPPING OF DOUBLY CONNECTED REGIONS ONTO A DISK WITH A SLIT

Ali H.M. Murid[1], Laey-Nee Hu[2] §
[1,2]Department of Mathematics
Faculty of Science
University of Technology – Malaysia
81310, UTM Skudai, Johor Darul Ta'zim, MALAYSIA
[1]e-mail: alihassan@utm.my
[2]e-mail: huln1234@yahoo.com.my

Abstract: We present a method for computing the conformal mapping function f of doubly connected regions bounded by two closed Jordan curves onto a disk with a concentric circular slit of radius $\mu < r$. Our mapping procedure consists of two parts. First we solve a system of integral equations on the boundary of the region we wish to map. The system of integral equations is based on a boundary integral equation involving the Neumann kernel discovered by the authors satisfied by $f'(z)$, $f'(a)$, r and μ, where a is a fixed interior point with $f'(a)$ predetermined. The boundary values of $f(z)$ are completely determined from the boundary values of $f'(z)$ through a boundary relationship. Discretization of the integral equation leads to a system of non-linear equations. Together with some normalizing conditions, a unique solution to the system is then computed by means of an optimization method called the Lavenberg-Marquadt algorithm. Once we have determined the boundary values of $f(z)$, we use the Cauchy integral formula to compute the interior of the regions. Typical examples for some doubly connected regions show that numerical results of high accuracy can be obtained for the conformal mapping problem when the boundaries are sufficiently smooth.

AMS Subject Classification: 30C30, 65R20, 65E05, 30C40, 65H10
Key Words: conformal mapping, integral equations, doubly connected re-

Received: February 26, 2009

§Correspondence author

gion, Neumann kernel, Lavenberg-Marquardt algorithm, Cauchy's integral formula

1. Introduction

Numerical conformal mapping of doubly connected regions are pre-sently still a subject of interest. Several methods for conformal mapping of doubly connected regions have been proposed in the literature (see [1], [4], [8], [12], [13], [15], [16] and [19]). One of the methods is the integral equation method. Some notable ones are the integral equations of Warschawski, Gerschgorin, and Symm. All these integral equations are extensions of those maps for simply connected regions. Recently, conformal mapping of doubly connected regions onto an annulus via the Kerzman-Stein is also discussed in Murid and Mohamed [12]. Murid and Hu [11] have also discussed numerical conformal mapping of multiply connected regions onto an annulus with circular slits via the Neumann kernel. But Murid and Razali [13], Murid and Mohamed [12] and Murid and Hu [11] have not yet formulated an integral equation method based on the Kerzman-Stein and the Neumann kernel for conformal mapping of doubly connected regions onto a disk with a circular slit.

The plan of the paper is as follows: In Section 2, we derive the system of two boundary integral equations involving the Neumann kernel for conformal mapping of doubly connected regions onto a disk $|w| \leq r$ with a circular slit of radius μr, with $0 < \mu < 1$. The system however involved the unknowns μ and r. In Section 3 we explain how to treat the system of integral equation numerically. The discretizetion of the integral equations leads to a system of non-linear equations which is then solved using the optimization method. The computation of the interior of the regions is shown in Section 4. In Section 5 we report our numerical results for some test regions and we draw some conclusions in Section 6.

2. The Boundary Integral Equation for Doubly Connected Region With Neumann Kernel

Let Γ_0 and Γ_1 be two smooth Jordan curves in the complex z-plane such that Γ_1 lies in the interior of Γ_0. Denote by Ω the finite doubly connected regions with boundary $\Gamma = \Gamma_0 \cup \Gamma_1$.

It is well known that if h is analytic and single-valued in Ω and continuous on $\Omega \cup \Gamma$, we have [7, p. 176]

$$\mathrm{PV}\frac{1}{2\pi \mathrm{i}} \int_{\Gamma} \frac{h(w)}{w-z} dw = \frac{1}{2} h(z), \quad z \in \Gamma. \tag{1}$$

Suppose $D(z)$ is analytic and single-valued with respect to $z \in \Omega$ and is continuous on $\Omega \cup \Gamma$. Suppose further that D satisfies the boundary relationship

$$D(z) = c(z) \left[\frac{T(z)Q(z)D(z)}{P(z)} \right]^{-}, \quad z \in \Gamma, \tag{2}$$

where the minus sign in the superscript denotes complex conjugation, $T(z) = z'(t)/|z'(t)|$ is the complex unit tangent function at $z \in \Gamma$, while c, P, and Q are complex-valued functions defined on Γ with the following properties:

(P1) $P(z)$ is analytic and single-valued with respect to $z \in \Omega$,

(P2) $P(z)$ is continuous on $\Omega \cup \Gamma$,

(P3) $P(z)$ has a finite number of zeroes at $a_1, a_2, ..., a_M$ in Ω,

(P4) $c(z) \neq 0, P(z) \neq 0, Q(z) \neq 0, D(z) \neq 0, z \in \Gamma$.

Note that the boundary relationship (2) also has the following equivalent form:

$$P(z) = \overline{c(z)} \frac{T(z)Q(z)D(z)^2}{|D(z)|^2}, \quad z \in \Gamma. \tag{3}$$

By means of (1), Murid and Hu [11] have shown that an integral equation for D may be constructed that is related to the boundary relationship (2):

Theorem 1. *Let u and v be any complex-valued functions that are defined on Γ. Then*

$$\frac{1}{2} \left[v(z) + \frac{u(z)}{\overline{T(z)Q(z)}} \right] D(z) + \mathrm{PV}\frac{1}{2\pi \mathrm{i}} \int_{\Gamma} \left[\frac{c(z)u(z)}{c(w)(\overline{w}-\overline{z})\overline{Q(w)}} - \frac{v(z)T(w)}{w-z} \right]$$

$$\times D(w)|dw| = -c(z)u(z) \left[\sum_{a_j inside \Gamma} \mathrm{Res}_{w=a_j} \frac{D(w)}{(w-z)P(w)} \right]^{-}, \quad z \in \Gamma, \tag{4}$$

where the minus sign in the superscript denotes complex conjugation.

Let $w = f(z)$ be the analytic function which maps Ω conformally onto a disk $|w| < r$ with circular slit of radius μr, where $0 < \mu < 1$. The function f could be made unique by prescribing that

$$f(a) = 0, \quad f'(a) > 0,$$

where $a \in \Omega$ is a fixed point.

The boundary value of f can be represented in form

$$f(z_0(t)) = re^{\mathrm{i}\theta_0(t)}, \quad \Gamma_0 : z = z_0(t), \quad 0 \le t \le \beta_0, \tag{5}$$

$$f(z_1(t)) = \mu re^{\mathrm{i}\theta_1(t)}, \ \Gamma_1 : z = z_1(t), \quad 0 \le t \le \beta_1, \tag{6}$$

where $\theta_0(t)$ and $\theta_1(t)$ are the boundary correspondence functions of Γ_0 and Γ_1 respectively.

The unit tangent to Γ at $z(t)$ is denoted by $T(z(t)) = z'(t)/|z'(t)|$. Thus it can be shown that

$$f(z_0(t)) = \frac{r}{\mathrm{i}} T(z_0(t)) \frac{\theta_0'(t)}{|\theta_0'(t)|} \frac{f'(z_0(t))}{|f'(z_0(t))|} = \frac{r}{\mathrm{i}} T(z_0(t)) \frac{f'(z_0(t))}{|f'(z_0(t))|}, \tag{7}$$

$$f(z_1(t)) = \frac{\mu r}{\mathrm{i}} T(z_1(t)) \frac{\theta_1'(t)}{|\theta_1'(t)|} \frac{f'(z_1(t))}{|f'(z_1(t))|} = \pm \frac{\mu r}{\mathrm{i}} T(z_1(t)) \frac{f'(z_1(t))}{|f'(z_1(t))|}. \tag{8}$$

Note that $\theta_0'(t) > 0$ while $\theta_1'(t)$ may be positive or negative since the circular slit $f(\Gamma_1)$ is traversed twice. Thus $\theta_1'(t)/|\theta_1'(t)| = \pm 1$.

The boundary relationships (7) and (8) can be unified as

$$f(z) = \pm \frac{|f(z)|}{\mathrm{i}} T(z) \frac{f'(z)}{|f'(z)|}, \quad z \in \Gamma, \tag{9}$$

where $\Gamma = \Gamma_0 \cup \Gamma_1$. Note that the value of $|f(z)|$ is either r or μr for $z \in \Gamma$. However we cannot compare (9) with (3) due to the presence of the $\pm$ sign. To overcome this problem, we square both sides of the boundary relationship (9) to get

$$f(z)^2 = -|f(z)|^2 T(z)^2 \frac{f'(z)^2}{|f'(z)|^2}, \quad z \in \Gamma. \tag{10}$$

Comparing (10) with (3), leads to a choice of $c(z) = -|f(z)|^2$, $P(z) = f(z)^2$, $D(z) = f'(z)$, $Q(z) = T(z)$, $u(z) = \overline{T(z)Q(z)}$ and $v(z) = 1$. Substituting these assignments into (4) leads to an integral equation satisfied by $f'(z)$, i.e.,

$$f'(z) + \mathrm{PV} \frac{1}{2\pi \mathrm{i}} \int_\Gamma \left[\frac{|f(z)|^2 \overline{T(z)^2}}{|f(w)|^2 (\overline{w} - \overline{z}) \overline{T(w)}} - \frac{T(w)}{(w - z)} \right] f'(w) |dw|$$

$$= |f(z)|^2 \overline{T(z)^2} \left[\sum_{a_j inside \Gamma} \operatorname*{Res}_{w=a_j} \frac{f'(w)}{(w - z) f(w)^2} \right]^{-}, \quad z \in \Gamma. \tag{11}$$

To evaluate the residue in equation (11) we use the fact that if $f(w) = g(w)/h(w)$ where g and h are analytic at a, and $g(a) \neq 0$, $h(a) = h'(a) = 0$, $h''(a) \neq 0$, which means a is a double pole of $f(w)$, then (see [5])

$$\operatorname*{Res}_{w=a} f(w) = 2 \frac{g'(a)}{h''(a)} - \frac{2}{3} \frac{h'''(a) g(a)}{h''(a)^2}. \tag{12}$$

Applying (12) and after several algebraic manipulations, we obtain

$$\operatorname*{Res}_{w=a} \frac{f'(w)}{(w-z)f(w)^2} = -\frac{1}{(a-z)^2 f'(a)}. \tag{13}$$

Thus integral equation (11) becomes

$$f'(z) + \mathrm{PV}\frac{1}{2\pi \mathrm{i}} \int_\Gamma \left[\frac{|f(z)|^2 \overline{T(z)^2}}{|f(w)|^2(\overline{w}-\overline{z})\overline{T(w)}} - \frac{T(w)}{(w-z)} \right] f'(w)|dw|$$

$$= -|f(z)|^2 \frac{\overline{T(z)^2}}{(\overline{a}-\overline{z})^2 f'(a)}, \qquad z \in \Gamma. \tag{14}$$

Multiply both sides by $f'(a)T(z)$ and use the fact $T(z)\overline{T(z)} = |T(z)|^2 = 1$ gives

$$f'(a)T(z)f'(z) + \mathrm{PV}\frac{1}{2\pi \mathrm{i}} \int_\Gamma \left[\frac{|f(z)|^2 \overline{T(z)}}{|f(w)|^2(\overline{w}-\overline{z})} - \frac{T(z)}{(w-z)} \right] f'(a)T(w)f'(w)|dw|$$

$$= -|f(z)|^2 \frac{\overline{T(z)}}{(\overline{a}-\overline{z})^2}, \qquad z \in \Gamma. \tag{15}$$

Equation (15) can also written as

$$g(z,a) + \int_\Gamma N^*(z,w)g(w,a)|dw| = |f(z)|^2 h(a,z), \qquad z \in \Gamma\,, \tag{16}$$

where

$$\begin{aligned} g(z,a) &= f'(a)T(z)f'(z), \qquad h(a,z) = -\frac{\overline{T(z)}}{(\overline{a}-\overline{z})^2}, \\ N^*(z,w) &= \frac{1}{2\pi \mathrm{i}} \left[\frac{T(z)}{(z-w)} - \frac{|f(z)|^2 \overline{T(z)}}{|f(w)|^2(\overline{z}-\overline{w})} \right]. \end{aligned}$$

For the doubly connected region map onto a circle with a concentric circular slit, the single integral equation in (16) can be separated into a system of equations

$$\begin{aligned} g(z_0,a) &+ \int_{\Gamma_0} N(z_0,w)g(w,a)|dw| - \int_{-\Gamma_1} P(z_0,w)g(w,a)|dw| \\ &= r^2 h(a,z_0), \quad z_0 \in \Gamma_0, \end{aligned} \tag{17}$$

$$\begin{aligned} g(z_1,a) &+ \int_{\Gamma_0} Q(z_1,w)g(w,a)|dw| - \int_{-\Gamma_1} N(z_1,w)g(w,a)|dw| \\ &= \mu^2 r^2 h(a,z_1), \quad z_1 \in \Gamma_1, \end{aligned} \tag{18}$$

where

$$P(z,w) = \frac{1}{2\pi \mathrm{i}} \left[\frac{T(z)}{(z-w)} - \frac{\overline{T(z)}}{\mu^2(\overline{z}-\overline{w})} \right],$$

$$Q(z,w) = \frac{1}{2\pi \mathrm{i}}\left[\frac{T(z)}{(z-w)} - \frac{\mu^2\overline{T(z)}}{(\overline{z}-\overline{w})}\right],$$

$$N(z,w) = \begin{cases} \dfrac{1}{2\pi \mathrm{i}}\left[\dfrac{T(z)}{z-w} - \dfrac{\overline{T(z)}}{\overline{z}-\overline{w}}\right], & \text{if } w,z \in \Gamma, w \neq z, \\ \dfrac{1}{2\pi}\dfrac{\mathrm{Im}[z''(t)\overline{z'(t)}]}{|z'(t)|^3}, & \text{if } w = z \in \Gamma. \end{cases}$$

The kernel N is also known as Neumann kernel.

Note that there are four unknown quantities in the integral equations (17) and (18), namely, $f'(a)T(z_0)f'(z_0)$, $f'(a)T(z_1)f'(z_1)$, r and μ. Naturally it is also required that the unknown mapping function $f(z)$ be single-valued in the problem domain [6], i.e.

$$\int_{-\Gamma_1} f'(w)dw = 0, \tag{19}$$

which implies

$$\int_{-\Gamma_1} g(w,a)|dw| = 0. \tag{20}$$

Several conditions can be obtained to help achieve uniqueness. We first consider equation (5). Upon differentiation and taking modulus to both sides of equation (5), gives

$$\begin{aligned} |f'(a)T(z_0(t))f'(z_0(t))z_0'(t)| &= |f'(a)T(z_0(t))re^{\mathrm{i}\theta_0(t)}\mathrm{i}\theta_0'(t)| \\ &= f'(a)r|\theta_0'(t)|. \end{aligned} \tag{21}$$

Since the boundary correspondence function $\theta_0(t)$ is an increasing monotone function its derivative is positive which implies $|\theta_0'(t)| = \theta_0'(t)$. Upon integrating (21) with respect to t form 0 to 2π gives

$$\int_0^{2\pi} |g(z_0(t),a)z_0'(t)|dt = f'(a)r\int_0^{2\pi} \theta_0'(t)dt = f'(a)r2\pi. \tag{22}$$

Next we consider the Cauchy integral formula

$$f'(a) = \frac{1}{2\pi \mathrm{i}}\int_\Gamma \frac{f'(z)}{z-a}dz, \tag{23}$$

which implies

$$f'(a)^2 = \frac{1}{2\pi \mathrm{i}}\int_0^{2\pi} \frac{f'(a)f'(z_0(t))z_0'(t)}{z_0(t)-a}dt - \frac{1}{2\pi \mathrm{i}}\int_0^{2\pi} \frac{f'(a)f'(z_1(t))z_1'(t)}{z_1(t)-a}dt. \tag{24}$$

Thus the system of integral equations comprising of (17), (18), (20) with the conditions (22) and (24) should lead to a unique solution.

3. Numerical Implementation

Using the parametric representations $z_0(t)$ of Γ_0 for $t : 0 \le t \le \beta_0$ and $z_1(t)$ of $-\Gamma_1$ for $t : 0 \le t \le \beta_1$ the system of integral equation (17), (18) and (20) becomes

$$g(z_0(t),a) + \int_0^{\beta_0} N(z_0(t),z_0(s))g(z_0(s),a)|z_0'(s)|ds - \int_0^{\beta_1} P(z_0(t),z_1(s))g(z_1(s),a)|z_1'(s)|ds = r^2 h(a,z_0(t)), \quad z_0(t) \in \Gamma_0, \quad (25)$$

$$g(z_1(t),a) + \int_0^{\beta_0} Q(z_1(t),z_0(s))g(z_0(s),a)|z_0'(s)|ds - \int_0^{\beta_1} N(z_1(t),z_1(s))g(z_1(s),a)|z_1'(s)|ds = r^2\mu^2 h(a,z_1(t)), \quad z_1(t) \in \Gamma_1, \quad (26)$$

$$\int_0^{\beta_1} g(z_1(s),a)|z_1'(s)|ds = 0. \quad (27)$$

Multipling (25) and (26) respectively by $|z_0'(t)|$ and $|z_1'(t)|$ gives

$$|z_0'(t)|g(z_0(t),a) + \int_0^{\beta_0} |z_0'(t)|N(z_0(t),z_0(s))g(z_0(s),a)|z_0'(s)|ds - \int_0^{\beta_1} |z_0'(t)|P(z_0(t),z_1(s))g(z_1(s),a)|z_1'(s)|ds = r^2|z_0'(t)|h(a,z_0(t)), \quad z_0(t) \in \Gamma_0, \quad (28)$$

$$|z_1'(t)|g(z_1(t),a) + \int_0^{\beta_0} |z_1'(t)|Q(z_1(t),z_0(s))g(z_0(s),a)|z_0'(s)|ds - \int_0^{\beta_1} |z_1'(t)|N(z_1(t),z_1(s))g(z_1(s),a)|z_1'(s)|ds = r^2\mu^2|z_1'(t)|h(a,z_1(t)), \quad z_1(t) \in \Gamma_1. \quad (29)$$

Defining

$$\phi_0(t) = |z_0'(t)|g(z_0(t),a), \qquad \phi_1(t) = |z_1'(t)|g(z_1(t),a),$$
$$\gamma_0(t) = r^2|z_0'(t)|h(a,z_0(t)), \qquad \gamma_1(t) = r^2\mu^2|z_1'(t)|h(a,z_1(t)),$$
$$K_{00}(t_0,s_0) = |z_0'(t)|N(z_0(t),z_0(s)), \qquad K_{01}(t_0,s_1) = |z_0'(t)|P(z_0(t),z_1(s)),$$
$$K_{10}(t_1,s_0) = |z_1'(t)|Q(z_1(t),z_0(s)), \qquad K_{11}(t_1,s_1) = |z_1'(t)|N(z_1(t),z_1(s)),$$

the system of equations (28), (29), (27), (22) and (24) can be briefly written as

$$\phi_0(t) + \int_0^{\beta_0} K_{00}(t_0, s_0)\phi_0(s)ds - \int_0^{\beta_1} K_{01}(t_0, s_1)\phi_1(s)ds = \gamma_0(t), \tag{30}$$

$$\phi_1(t) + \int_0^{\beta_0} K_{10}(t_1, s_0)\phi_0(s)ds - \int_0^{\beta_1} K_{11}(t_1, s_1)\phi_1(s)ds = \gamma_1(t), \tag{31}$$

$$\int_0^{\beta_1} \phi_1(s)ds = 0, \tag{32}$$

$$\int_0^{\beta_0} |\phi_0(s)|ds = f'(a)r2\pi, \tag{33}$$

$$\frac{1}{2\pi \mathrm{i}} \int_0^{\beta_0} \frac{\phi_0(s)}{z_0(s) - a}ds - \frac{1}{2\pi \mathrm{i}} \int_0^{\beta_1} \frac{\phi_1(s)}{z_1(s) - a}ds = f'(a)^2. \tag{34}$$

Since the functions ϕ, γ, and K in the above systems are β-periodic, a reliabbe procedure for solving (30) to (34) numerically is using the Nyström's method with trapezoidal rule [2]. The trapezoidal rule is the most accurate method for integrating periodic functions numerically [3, pp. 134-142]. We choose $\beta_0 = \beta_1 = 2\pi$ and n equidistant collocation points $t_i = (i-1)\beta_0/n$, $1 \le i \le n$ on Γ_0 and m equidistant collocation points $t_{\tilde{i}} = (\tilde{i} - 1)\beta_1/m$, $1 \le \tilde{i} \le m$, on Γ_1. Applying the Nyström's method with trapezoidal rule to discretize (30) to (34), we obtain

$$\phi_0(t_i) + \frac{\beta_0}{n} \sum_{j=1}^{n} K_{00}(t_i, t_j)\phi_0(t_j) - \frac{\beta_1}{m} \sum_{\jmath=1}^{m} K_{01}(t_i, t_\jmath)\phi_1(t_\jmath) = \gamma_0(t_i), \tag{35}$$

$$\phi_1(t_\imath) + \frac{\beta_0}{n} \sum_{j=1}^{n} K_{10}(t_\imath, t_j)\phi_0(t_j) - \frac{\beta_1}{m} \sum_{\jmath=1}^{m} K_{11}(t_\imath, t_\jmath)\phi_1(t_\jmath) = \gamma_1(t_\imath), \tag{36}$$

$$\sum_{\jmath=1}^{m} \phi_1(t_\jmath) = 0, \tag{37}$$

$$\sum_{j=1}^{n} |\phi_0(t_j)| = f'(a)rn, \tag{38}$$

$$\frac{1}{n\mathrm{i}} \sum_{j=1}^{n} \frac{1}{z_0(t_j) - a}\phi_0(t_j) - \frac{1}{m\mathrm{i}} \sum_{\jmath=1}^{m} \frac{1}{z_1(t_\jmath) - a}\phi_1(t_\jmath) = f'(a)^2. \tag{39}$$

Equations (35) to (39) lead to a system of $(n + m + 3)$ non-linear complex equations in n unknowns $\phi_0(t_i)$, m unknowns $\phi_1(t_\imath)$, $f'(a)$, r and μ. By defining

the matrices

$$B_{ij} = \frac{\beta_0}{n} K_{00}(t_i, t_j), \qquad C_{ij} = \frac{\beta_1}{m} K_{01}(t_i, t_j),$$
$$E_{ij} = \frac{\beta_0}{n} K_{10}(t_i, t_j), \qquad D_{ij} = \frac{\beta_1}{m} K_{11}(t_i, t_j),$$
$$F_j = \frac{1}{\mathrm{i}n} \sum_{j=1}^{n} \frac{1}{z_0(t_j) - a}, \qquad G_j = \frac{1}{\mathrm{i}m} \sum_{j=1}^{m} \frac{1}{z_1(t_j) - a},$$
$$x_{0i} = \phi_0(t_i), \qquad x_{1i} = \phi_1(t_i),$$
$$\gamma_{0i} = \gamma_0(t_i), \qquad \gamma_{1i} = \gamma_1(t_i),$$

the system of equations (35), (36) and (39) can be written as $n + m + 1$ by $n + m$ system of equations

$$[I_{nn} + B_{nn}]\mathbf{x}_{0n} - C_{nm}\mathbf{x}_{1m} = \gamma_{0n}, \tag{40}$$
$$E_{mn}\mathbf{x}_{0n} + [I_{mm} - D_{mm}]\mathbf{x}_{1m} = \gamma_{1m}, \tag{41}$$
$$F_n\mathbf{x}_{0n} + G_m\mathbf{x}_{1m} = f'(a)^2. \tag{42}$$

Since $\phi = \mathrm{Re}\phi + \mathrm{iIm}\phi$, equations (37) and (38) become

$$\sum_{j=1}^{m} (\mathrm{Re}x_{1j} + \mathrm{iIm}x_{1j}) = 0, \tag{43}$$

$$\sum_{j=1}^{n} \sqrt{(\mathrm{Re}x_{0j})^2 + (\mathrm{Im}x_{0j})^2} = f'(a)rn. \tag{44}$$

The result in matrix form for the system of equations (40), (41) and (42) is

$$\begin{pmatrix} I_{nn} + B_{nn} & \cdots & -C_{nm} \\ \vdots & \ddots & \vdots \\ E_{mn} & \cdots & I_{mm} - D_{mm} \\ \vdots & \ddots & \vdots \\ F_n & \cdots & G_m \end{pmatrix} \begin{pmatrix} \mathbf{x}_{0n} \\ \vdots \\ \mathbf{x}_{1m} \end{pmatrix} = \begin{pmatrix} \gamma_{0n} \\ \vdots \\ \gamma_{1m} \\ \vdots \\ f'(a)^2 \end{pmatrix}. \tag{45}$$

Defining

$$A = \begin{pmatrix} I_{nn} + B_{nn} & \cdots & -C_{nm} \\ \vdots & \ddots & \vdots \\ E_{mn} & \cdots & I_{mm} - D_{mm} \\ \vdots & \ddots & \vdots \\ F_n & \cdots & G_m \end{pmatrix}, \ \mathbf{x} = \begin{pmatrix} \mathbf{x}_{0n} \\ \vdots \\ \mathbf{x}_{1m} \end{pmatrix} \text{ and } \mathbf{y} = \begin{pmatrix} \gamma_{0n} \\ \vdots \\ \gamma_{1m} \\ \vdots \\ f'(a)^2 \end{pmatrix},$$

the $(n+m+1) \times (n+m)$ system can be written briefly as $A\mathbf{x} = \mathbf{y}$. Separating A, $\mathbf{x}$ and $\mathbf{y}$ in terms of the real and imaginary parts, the system can be written

as

$$\mathrm{Re\,A\,Re\,x} - \mathrm{Im\,AIm\,x} + \mathrm{i}(\,\mathrm{ImARe\,x} + \mathrm{Re\,A\,Im\,x}) = \mathrm{Re\,y} + \mathrm{iIm\,y}. \tag{46}$$

The single $(n+m+1)\times(n+m)$ complex system (46) above is equivalent to the $2(n+m+1)\times 2(n+m)$ system matrix involving the real (Re) and imaginary (Im) of the unknown functions, i.e.,

$$\begin{pmatrix} \mathrm{Re\,A} & \cdots & \mathrm{Im\,A} \\ \vdots & \ddots & \vdots \\ \mathrm{Im\,A} & \cdots & \mathrm{Re\,A} \end{pmatrix} \begin{pmatrix} \mathrm{Re\,x} \\ \vdots \\ \mathrm{Im\,x} \end{pmatrix} = \begin{pmatrix} \mathrm{Re\,y} \\ \vdots \\ \mathrm{Im\,y} \end{pmatrix}. \tag{47}$$

Note that the matrix in (47) contains the unknown parameters r and μ. The value of $f'(a)$ is predetermined. The system of equations (47), (43) and (54) is an over-determined system of non-linear equations involving $2(n+m+1)+2$ equations in $2(n+m)+2$ unknowns.

Methods for solving over-determined system are best dealt with as problems in optimization [24, p. 146]. We use a modification of the Gauss-Newton called the Lavenberg-Marquardt with the Fletcher's algorithm [22, pp. 233-246] to solve this nonlinear least square problem. Our nonlinear least square problem consists in finding the vector $\mathbf{x}$ for which the function $S : R^{2(n+m)+4} \to R^1$ defined by the sum of squares

$$S(\mathbf{x}) = \mathbf{f}^{\mathrm{T}}\mathbf{f} = \sum_{i=1}^{2(n+m)+4} (f_i(\mathbf{x}))^2$$

is minimal. Here, $\mathbf{x}$ stands for the $2(n+m)+2$ vector ($\mathrm{Re}\,x_{01}$, $\mathrm{Re}\,x_{02}$, ..., $\mathrm{Re}\,x_{0n}$, $\mathrm{Re}\,x_{11}$, $\mathrm{Re}\,x_{12}$, ..., $\mathrm{Re}\,x_{1m}$, $\mathrm{Im}\,x_{01}$, $\mathrm{Im}\,x_{02}$, ..., $\mathrm{Im}\,x_{0n}$, $\mathrm{Im}\,x_{11}$, $\mathrm{Im}\,x_{12}$, ..., $\mathrm{Im}\,x_{1m}$, μ, r), and $\mathbf{f} = (f_1, f_2, ..., f_{2(n+m)+4})$. The Lavenberg-Marquardt algorithm is an iterative procedure with starting value denoted as $\mathbf{x}_0$. This initial approximation, which, if at all possible, should be well-informed guess and generate a sequence of approximations $\mathbf{x}_1$, $\mathbf{x}_2$, $\mathbf{x}_3$, ... based on the formula

$$\mathbf{x}_{k+1} = \mathbf{x}_k - H(\mathbf{x}_k)\mathbf{f}(\mathbf{x}_k), \qquad \lambda_k \geq 0, \tag{48}$$

where $H(\mathbf{x}_k) = ((J_{\mathbf{f}}(\mathbf{x}_k))^T J_{\mathbf{f}}(\mathbf{x}_k) + \lambda_k I)^{-1}(J_{\mathbf{f}}(\mathbf{x}_k))^T$.

The strategy for getting the initial estimation is to provide rough estimates of the slit radius, $\mu \approx 0.5$, $r = 1$ and set $f'(a) = 1$ for the test region. Then the non-linear system of equations (47) and (43) reduces to over-determined linear system. Writing the over-determined system as $\mathrm{B}\mathbf{x} = \mathbf{y}$, we use the least-squares solutions of $\mathrm{B}\mathbf{x} = \mathbf{y}$ which are precisely the solutions of $\mathrm{B}^{\mathrm{T}}\mathrm{B}\mathbf{x} = \mathrm{B}^{\mathrm{T}}\mathbf{y}$, see [9]. The solutions are then taken as initial estimation. These initial guesses are applied for the lowest number of n and m of our experiments. In all our experiments, we have chosen the number of collocation points on Γ_0 and Γ_1

being equal, i.e., $n = m$. The information from the solution of μ and r of lower n is then exploited as an estimate of μ and r for the next $2n$ number of collocations points.

The system of equations (47) with (43) and (54) are then solved for the unknown function

$$\phi_0(t) = |z_0'(t)|f'(a)T(z_0(t))f'(z_0(t)),$$
$$\phi_1(t) = |z_1'(t)|f'(a)T(z_1(t))f'(z_1(t)),$$

μ and r. Finally the boundary correspondence functions $\theta_0(t)$ and $\theta_1(t)$ are computed approximately by the formulas

$$\theta_0(t) = \operatorname{Arg} f(z_0(t)) \approx \operatorname{Arg}(-\mathrm{i}\phi_0(t)),$$
$$\theta_1(t) = \operatorname{Arg} f(z_1(t)) \approx \operatorname{Arg}(\pm\mathrm{i}\phi_1(t)).$$

4. The Interior of Doubly Connected Regions

Once the boundary values of the mapping function f are known, the values of the mapping function may be calculated by quadrature at any interior points of its domain of definition through Cauchy's integral formula for doubly connected region which read as follows:

Theorem 2. (Cauchy's Integral Formula) *Let f be analytic on the boundaries $\Gamma = \Gamma_0 \cup \Gamma_1$ and the region Ω bounded by Γ_0 and Γ_1. If ζ is any point on Ω, then*

$$f(\zeta) = \frac{1}{2\pi\mathrm{i}}\int_{\Gamma}\frac{f(z)}{z-\zeta}dz = \frac{1}{2\pi\mathrm{i}}\int_{\Gamma_0}\frac{f(z)}{z-\zeta}dz - \frac{1}{2\pi\mathrm{i}}\int_{-\Gamma_1}\frac{f(z)}{z-\zeta}dz. \quad (49)$$

The Cauchy's integral formula (49) can be also written in the parametrized form, i.e.

$$f(\zeta) = \frac{1}{2\pi\mathrm{i}}\int_0^{\beta_0}\frac{f(z_0(t))z_0'(t)}{z_0(t)-\zeta}dt - \frac{1}{2\pi\mathrm{i}}\int_0^{\beta_1}\frac{f(z_1(t))z_1'(t)}{z_1(t)-\zeta}dt. \quad (50)$$

By means of (5) and (6), the Cauchy's integral formula (49) can then be written in the form

$$f(\zeta) = \frac{1}{2\pi\mathrm{i}}\int_0^{\beta_0}\frac{re^{\mathrm{i}\theta_0(t)}z_0'(t)}{z_0(t)-\zeta}dt - \frac{1}{2\pi\mathrm{i}}\int_0^{\beta_1}\frac{\mu re^{\mathrm{i}\theta_1(t)}z_1'(t)}{z_1(t)-\zeta}dt. \quad (51)$$

For the points which are not close to the boundary, the integrands are well behaved. However for points near the boundary, the numerical integration is inaccurate due to the influence of the singularity. This difficulty is overcome

through the introduction of an iterative technique as given in [18, p. 303]. If we define $f_0(\zeta)$ to be $f(z)$ where z is a point on the boundary which is closest to ζ, then we can define

$$f_{k+1}(\zeta) = \frac{1}{2\pi \mathrm{i}} \int_\Gamma \frac{f(z) - f_k(\zeta)}{z - \zeta} dz + f_k(\zeta). \tag{52}$$

In practice the iteration converges rapidly. Using this technique, we are able to maintain the same accuracy throughout the region Ω.

5. Numerical Results

For numerical experiments, we have used five test regions whose exact boundary correspondence functions are known. The test regions are annulus, frame of Limacon, elliptic frame, circular frame and frame of Cassini's oval. We set $f'(a) = 1$ for all test regions. Note that, $f(z)$ maps Ω conformally onto a disk $|w| < r$ with a circular slit of radius μr, where $0 < \mu < 1$. Thus $g(z) = f(z)/r$ maps Ω onto a disk $|w| < 1$ with a circular slit of radius μ. This implies that f and g have the same values of $\theta_0(t)$, $\theta_1(t)$ and μ. The results for the sub-norm error between the exact values of $\theta_0(t)$, $\theta_1(t)$, μ and their corresponding approximations $\theta_{0n}(t)$, $\theta_{1n}(t)$, μ_n are shown in Tables 1 to 5. All the computations are done using *Mathematica* package [23] in single precision (16 digit machine precision).

Example 3. (Annulus) Consider a frame of circular annulus $A = \{z : \tilde{r} < |z| < 1\}$, $\tilde{r} = q = e^{-\pi\tau}$, $\tau > 0$.

$$\begin{aligned} \Gamma_0 : \{z(t) &= \cos t + \mathrm{i} \sin t\}, \\ \Gamma_1 : \{z(t) &= \tilde{r}(\cos t + \mathrm{i} \sin t)\}. \end{aligned}$$

The exact mapping function that maps A onto unit disk with a circular slit is given by [20]

$$g(z) = -e^{2\sigma} \frac{\theta_4\left(\frac{1}{2\mathrm{i}} \log z + \frac{\mathrm{i}\pi\tau}{2} - \mathrm{i}\sigma\right)}{\theta_4\left(\frac{1}{2\mathrm{i}} \log z + \frac{\mathrm{i}\pi\tau}{2} + \mathrm{i}\sigma\right)}, \qquad 0 < \sigma < \frac{\pi\tau}{2}, \tag{53}$$

with $\mu = e^{-2\sigma}$ and θ_4 being the Jacobi Theta-functions. We have chosen $\tau = 0.50$ and $\sigma = 0.20$. Since $\theta_4(\pi\tau\mathrm{i}/2) = 0$ [21], this implies $a = e^{-2\sigma} = \mu$. Figure 1 shows the region and image based on our method. See Table 1 for results.

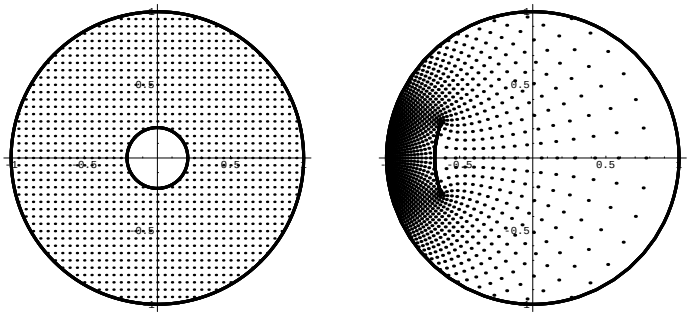

Figure 1: Annulus: A rectangular grid in Ω with grid size 0.05 and its image with $\tau = 0.50, \sigma = 0.20, \tilde{r} = e^{-\pi\tau}$ and $a = e^{-2\sigma}$

$n = m$	$\|\theta_0(t) - \theta_{0n}(t)\|_\infty$	$\|\theta_1(t) - \theta_{1n}(t)\|_\infty$	$\|\mu - \mu_n\|_\infty$
16	1.9(−02)	6.3(−01)	1.7(−02)
32	5.0(−05)	8.9(−04)	2.8(−05)
64	2.4(−10)	2.3(−09)	8.2(−11)
128	8.9(−16)	7.0(−14)	2.2(−16)

Table 1: Error norm (annulus)

Example 4. (Circular Frame) Consider a pair of circles [17]

$$\begin{aligned} \Gamma_0 : \{z(t) &= e^{\mathrm{i}t}\}, \\ \Gamma_1 : \{z(t) &= c + \rho e^{\mathrm{i}t}\}, \qquad t : 0 \le t \le 2\pi\,, \end{aligned}$$

such that the domain bounded by Γ_0 and Γ_1 is the domain between a unit circle and a circle center at c with radius ρ. Since $\theta_4(\pi\tau\mathrm{i}/2) = 0$ and $\tilde{r} = q = e^{-\pi\tau}$, this implies $\tau = \frac{\ln(\tilde{r})}{-\pi}$ and $a = \frac{\lambda - e^{-2\sigma}}{1 - \lambda e^{-2\sigma}}$. We choose a real number σ such that $0 < \sigma < \pi\tau/2$. Then the exact mapping function is given by

$$g(z) = e^{2\sigma} \frac{\theta_4\left(\dfrac{1}{2\mathrm{i}} \log p(z) + \dfrac{\mathrm{i}\pi\tau}{2} - \mathrm{i}\sigma\right)}{\theta_4\left(\dfrac{1}{2\mathrm{i}} \log p(z) + \dfrac{\mathrm{i}\pi\tau}{2} + \mathrm{i}\sigma\right)}, \qquad 0 < \sigma < \frac{\pi\tau}{2}, \tag{54}$$

where $p(z) = (z - \lambda)/(\lambda z - 1)$ with

$$\lambda = \frac{2c}{1 + (c^2 - \rho^2) + \sqrt{(1 - (c - \rho)^2)(1 - (c + \rho)^2)}},$$

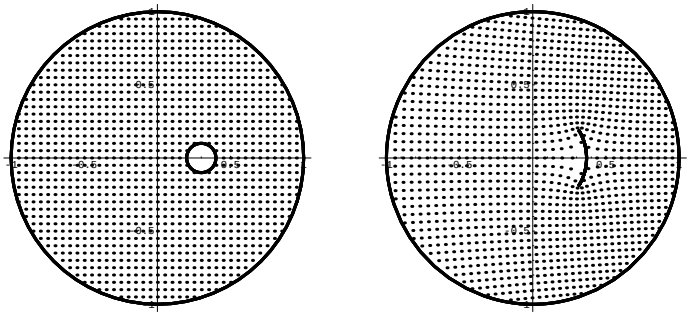

Figure 2: Circular frame: A rectangular grid in Ω with grid size 0.05 and its image with $c = 0.3, \rho = 0.1, \sigma = 0.50, \mu = e^{-2\sigma}$

$n = m$	$\|\theta_0(t) - \theta_{0n}(t)\|_\infty$	$\|\theta_1(t) - \theta_{1n}(t)\|_\infty$	$\|\mu - \mu_n\|_\infty$
4	1.0(−01)	5.9(−01)	4.9(−01)
8	2.3(−04)	2.0(−03)	1.6(−04)
16	1.0(−08)	4.2(−07)	2.0(−08)
32	8.9(−16)	5.1(−14)	1.8(−15)

Table 2: Error norm (circular frame)

$$\tilde{r} = \frac{2\rho}{1 - (c^2 - \rho^2) + \sqrt{(1 - (c - \rho)^2)(1 - (c + \rho)^2)}}.$$

Figure 2 shows the region and image based on our method. See Table 2 for results.

Example 5. (Frame of Limacon) Consider a pair of Limacon [10]:

$$\Gamma_0 : \{z(t) = a_0 \cos t + b_0 \cos 2t + \mathrm{i}(a_0 \sin t + b_0 \sin 2t),\ a_0 > 0, b_0 > 0\},$$
$$\Gamma_1 : \{z(t) = a_1 \cos t + b_1 \cos 2t + \mathrm{i}(a_1 \sin t + b_1 \sin 2t),\ a_1 > 0, b_1 > 0\},$$

with $a_0 = 10$, $a_1 = 5$, $b_0 = 3$ and $b_1 = b_0/4$ where $t : 0 \le t \le 2\pi$. The values of a_0, a_1, b_0 and b_1 are chosen so that $b_1/b_0 = a_1/a_0$ and $\tilde{r} = a_1/a_0$. Since $\theta_4(\pi\tau \mathrm{i}/2) = 0$ and $\tilde{r} = q = e^{-\pi\tau}$, this implies $\tau = \frac{\ln(a_1/a_0)}{-\pi}$ and $a = \frac{(2b_0 e^{-2\sigma} + a_0)^2 - a_0^2}{4b_0}$. We choose a real number σ satisfying $0 < \sigma < \pi\tau/2$. The

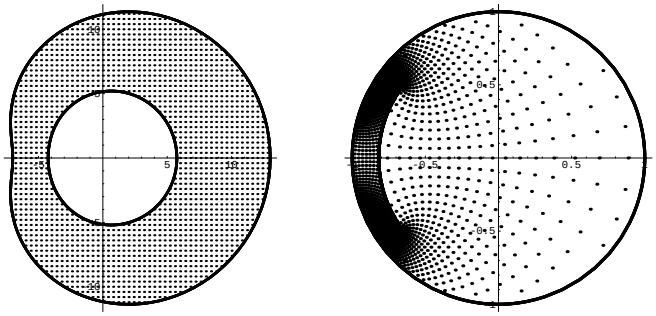

Figure 3: Frame of Limacons: A rectangular grid in Ω with grid size 0.4 and its image with $\sigma = 0.10$

$n = m$	$\|\theta_0(t) - \theta_{0n}(t)\|_\infty$	$\|\theta_1(t) - \theta_{1n}(t)\|_\infty$	$\|\mu - \mu_n\|_\infty$
32	2.5(−02)	4.0(−02)	6.9(−03)
64	6.3(−05)	2.4(−04)	1.5(−05)
128	2.9(−10)	3.8(−09)	5.8(−11)

Table 3: Error norm (frame of Limacon)

exact mapping function is given by

$$g(z) = -e^{2\sigma}\frac{\theta_4\left(\dfrac{1}{2\mathrm{i}}\log p(z) + \dfrac{\mathrm{i}\pi\tau}{2} - \mathrm{i}\sigma\right)}{\theta_4\left(\dfrac{1}{2\mathrm{i}}\log p(z) + \dfrac{\mathrm{i}\pi\tau}{2} + \mathrm{i}\sigma\right)}, \qquad 0 < \sigma < \frac{\pi\tau}{2}, \tag{55}$$

where $p(z) = \dfrac{\sqrt{a_0^2 + 4b_0 z} - a_0}{2b_0}, \mu = e^{-2\sigma}$. Figure 3 shows the region and image based on our method. See Table 3 for results.

Example 6. (Elliptic Frame) Elliptic frame is the domain bounded by two Jordan curves, Γ_0 and Γ_1 such that

$$\Omega : \frac{x^2}{a_0^2} + \frac{y^2}{b_0^2} < 1, \qquad \frac{x^2}{a_1^2} + \frac{y^2}{b_1^2} > 1,$$

with the complex parametric of its boundary is given by [1]

$$\begin{aligned} \Gamma_0 : \{z(t) &= a_0 \cos t + \mathrm{i}b_0 \sin t, a_0 > 0, b_0 > 0\}, \\ \Gamma_1 : \{z(t) &= a_1 \cos t + \mathrm{i}b_1 \sin t, a_1 > 0, b_1 > 0\}, \qquad 0 \le t \le 2\pi. \end{aligned}$$

Since $\theta_4(\pi\tau\mathrm{i}/2) = 0$ and $\tilde{r} = q = e^{-\pi\tau}$, this implies $\tau = -\ln(\tilde{r})/\pi$ and $a =$

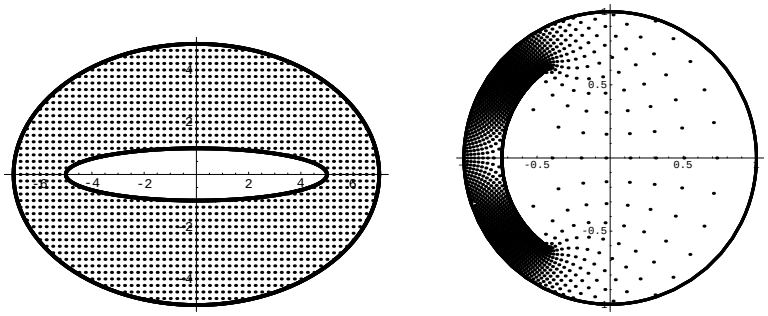

Figure 4: Elliptic frame: a rectangular grid in Ω with grid size 0.25 and its image with $a_0 = 7, a_1 = 5, b_0 = 5, b_1 = 1, \sigma = 0.10$

$n = m$	$\|\theta_0(t) - \theta_{0n}(t)\|_\infty$	$\|\theta_1(t) - \theta_{1n}(t)\|_\infty$	$\|\mu - \mu_n\|_\infty$
16	1.6(−01)	6.4(−01)	1.7(−02)
32	8.9(−04)	2.3(−03)	3.2(−04)
64	1.0(−07)	8.7(−07)	2.8(−08)
128	1.2(−14)	3.2(−13)	1.2(−14)

Table 4: Error norm (elliptic frame)

$\frac{e^{-4\sigma}(a_0+b_0)^2+(a_0-b_0)^2}{2e^{-2\sigma}(a_0+b_0)}$. The two ellipses Γ_0 and Γ_1 are confocal such that $a_0^2 - b_0^2 = a_1^2 - b_1^2$. We choose a real number σ satisfying $0 < \sigma < \pi\tau/2$. Then the exact mapping function is given by equation (55), where

$$p(z) = \frac{z + \sqrt{z^2 - (a_0^2 - b_0^2)}}{a_0 + b_0}, \qquad \tilde{r} = \frac{a_1 + b_1}{a_0 + b_0}, \qquad \mu = e^{-2\sigma}.$$

Figure 4 shows the region and image based on our method. See Table 4 for results.

Example 7. (Frame of Cassini's Oval) If Ω is the region bounded by two Cassini's oval, then the complex parametric equation of its boundary is given by [1]

$$\Gamma_0 : \{z(t) = \sqrt{b_0^2 \cos 2t + \sqrt{a_0^4 - b_0^4 \sin^2 2t}}\, e^{it}, a_0 > 0, b_0 > 0\},$$

$$\Gamma_1 : \{z(t) = \sqrt{b_1^2 \cos 2t + \sqrt{a_1^4 - b_1^4 \sin^2 2t}}\, e^{it}, a_1 > 0, b_1 > 0\}, \quad 0 \le t \le 2\pi.$$

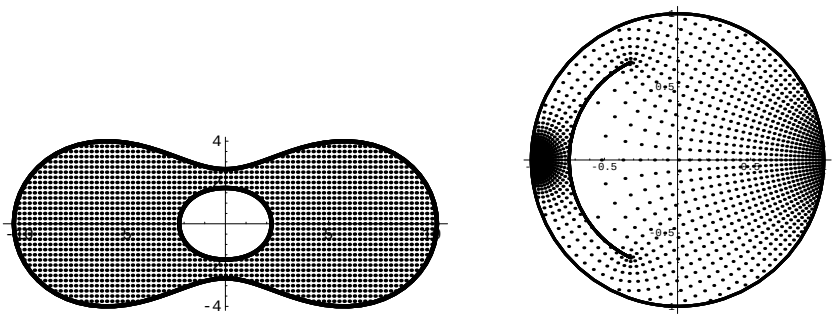

Figure 5: Frame of Cassini's oval: A rectangular grid in Ω with grid size 0.25 and its image with $a_0 = 2\sqrt{14}, a_1 = 2, b_0 = 7, b_1 = 1$ and $\sigma = 0.15$

$n = m$	$\|\theta_0(t) - \theta_{0n}(t)\|_\infty$	$\|\theta_1(t) - \theta_{1n}(t)\|_\infty$	$\|\mu - \mu_n\|_\infty$
32	4.0(−03)	5.0(−03)	6.0(−04)
64	1.0(−06)	1.1(−06)	1.2(−07)
128	4.9(−14)	7.5(−12)	8.4(−14)

Table 5: Error norm (frame of Cassini's oval)

such that

$$\Omega : |z^2 - b_0^2| < a_0^2, \qquad |z^2 - b_1^2| > a_1^2 \,.$$

Since $\theta_4(\pi\tau \mathrm{i}/2) = 0$, $\tilde{r} = q = e^{-\pi\tau}$ and $f'(a) > 0$, this implies $\tau = -\ln(\tilde{r})/\pi$ and $a = \sqrt{\frac{e^{-4\sigma}(a_0^4 - b_0^4)}{a_0^2 - b_0^2 e^{-4\sigma}}}$. The boundaries Γ_0 and Γ_1 are chosen such that $(a_0^4 - b_0^4)/b_0^2 = (a_1^4 - b_1^4)/b_1^2$. We choose a real number σ satisfying $0 < \sigma < \pi\tau/2$. Then the exact mapping function is given by equation (55), where

$$p(z) = \frac{a_0 z}{\sqrt{b_0^2 z^2 + a_0^4 - b_0^4}}, \qquad \tilde{r} = \frac{a_0 b_1}{a_1 b_0}, \qquad \mu = e^{-2\sigma}.$$

Figure 5 shows the region and image based on our method. See Table 5 for results.

6. Conclusion

In this paper we have constructed a system of integral equations for numerical conformal mapping from a doubly connected regions onto a disk of radius r

with a concentric circular slit of radius μr. The system involved the Neumann kernel and unknown parameters μ and r with $f'(a)$ predetermined. Due to the presence of μ in the kernel, the discretized integral equation leads to a system of nonlinear equations which is solved using optimization method. Several mappings of the test regions were computed numerically using the proposed method. The advantage of our method is that it calculates the boundary correspondence functions and the unknown parameters μ and r simultaneously with same degree of accuracy. Having computed the boundary values of the mapping function, the interior values are then calculated by means of the Cauchy integral formula. The numercial examples show the effectiveness of the proposed method.

Acknowledgements

This work was supported in part by the Malaysian Ministry of Higher Education (MOHE) through the Research Management Centre (RMC), University Technology Malaysia (FRGS Vote 78089). This support is gratefully acknowledged. The authors are indebted to Professor Rudolf Wegmann of Max-Planck-Institut, Garching, Germany for helpful discussions on the exact mapping function in Example 3 and for bringing reference [20] to our attention. The authors also wish to thank Professor Mohd Nor Mohamad of Department of Mathematics, Faculty of Science, University Technology Malaysia for fruitful discussions.

References

[1] K. Amano, A charge simulation method for the numerical conformal mapping of interior, exterior and doubly connected domains, *J. Comp. Appl. Math.*, **53** (1994), 353-370.

[2] K.E. Atkinson, *A Survey of Numerical Methods for the Solution of Fredholm Integral Equations,* Society for Industry and Applied Mathematics, Philadephia (1976).

[3] P.J. Davis, P. Rabinowitz, *Methods of Numerical Integration, Second Edition,* Academic Press, Orlando (1984).

[4] S.W. Ellacott, On the approximate conformal mapping of multiply connected domains, *Numerische Mathematik,* **33** (1979), 437-446.

[5] M.O. Gonzalez, *Classical Complex Analysis,* Marcel Decker, New York (1992).

[6] P. Henrici, *Applied and Computational Complex Analysis, Volume 3,* John Wiley, New York (1986).

[7] E. Hille, *Analytic Function Theory, Volume 1,* Chelsea, New York (1973).

[8] D.M. Hough, N. Papamichael, An integral equation method for the numerical conformal mapping of interior, exterior and doubly-connected domains, *Numerische Mathematik,* **14** (1983), 287-307.

[9] L.W. Johnson, R.D. Riess, J.T. Arnold, *Linear Algebra,* 4-th Edition, Addison-Wesley Longman, New York (1998).

[10] P.K. Kythe, *Computational Conformal Mapping,* Birkhäuser, Boston, New Orleans (1998).

[11] A.H.M. Murid, L.N. Hu, Numerical conformal mapping of bounded multiply connected regions by an integral equation method, *Int. J. Contemp. Math. Sciences,* Submited.

[12] A.H.M. Murid, N.A. Mohamed, An integral equation method for conformal mapping of doubly connected regions via the Kerzman-Stein kernel. *IJPAM,* **38**, No. 3 (2007), 229-250.

[13] A.H.M. Murid, M.R. M. Razali, An integral equation method for conformal mapping of doubly-connected regions, *Matematika,* **15**, No. 2 (1999), 79-93.

[14] Z. Nehari, *Conformal Mapping,* Dover Publications Inc., New York (1952).

[15] N. Papamicheal, M.K. Warby, Pole-type singularities and the numerical conformal mapping of doubly connected domains, *Journal of Comp. Appl. Math.,* **10** (1984), 93-106.

[16] N. Papamicheal, C.A. Kokkinos, The use of singular function for the approximate conformal mapping of doubly-connected domains, *SIAM J. Sci. Stst. Comput.,* **5**, No. 3 (1984), 684-700.

[17] E.B. Saff, A.D. Snider, *Fundamentals of Complex Analysis,* Pearson Education Inc., New Jersey (2003).

[18] P.N. Swarztrauber, On the numerical solution of the Dirichlet problem for a region of general shape, *SIAM J. Numer. Anal.,* **9**, No. 2 (1972), 300-306).

[19] G.T. Symm, Conformal mapping of doubly connected domain, *Numer. Math.,* **13** (1969), 448-457.

[20] W. von Koppenfels, F. Stallmann, *Praxis der Konformen Abbildung,* Göttingen, Heidelberg, Berlin (1959).

[21] E.T. Whittaker, G.N. Watson, *A Course of Modern Analysis,* University Press, Cambridge (1927).

[22] M.A. Wolfe, *Numerical Methods for Unconstrained Optimization,* Van Nostrand Reinhold Company, New Delhi (1978).

[23] S. Wolfram, *Mathematica: A System of Doing Mathematics by Computer,* Redwood City, Addison-Wesley (1991).

[24] C. Woodford, *Solving Linear, Non-Linear Equations,* McGraw-Hill, New York (1992).